Reconstruction of a large runout landslide in the Krušné hory Mts. (Czech Republic)

J. Burda, M. Veselý, M. Řehoř & V. Vilímek

Landslides
Journal of the International Consortium on Landslides

ISSN 1612-510X
Volume 15
Number 3

Landslides (2018) 15:423-437
DOI 10.1007/s10346-017-0881-0

Springer

Original Paper

Landslides (2018) 15:423–437
DOI 10.1007/s10346-017-0881-0
Received: 11 April 2017
Accepted: 11 August 2017
Published online: 25 August 2017

J. Burda · M. Veselý · M. Řehoř · V. Vilímek

Reconstruction of a large runout landslide in the Krušné hory Mts. (Czech Republic)

Abstract The aims of this study were to summarize current knowledge of a large runout prehistoric landslide, critically review all of the existing data and, in particular, gather new data in order to estimate the age of the accumulation and reveal the movement mechanism. The reconstruction of a large rockslide-rock avalanche in the NW part of the Czech Republic was supported by the analysis and interpretation of 216 boreholes and by GIS analysis of the original 1950s pre-mining surface using digitized old military topographic maps. For the age estimation, we used the Schmidt hammer test. The total volume of the quaternary deposit was calculated to be between 25.4 and 27.4 mil m^3, occupying an area of 778,000 m^2 and consisting of six to eight generations of colluvial sediments. Three main landslide events were identified based on extensive Schmidt hammer sampling, and the approximate age was established using a regression equation assembled by Engel (2007). All three of the documented events occurred around the time of significant climate change. The oldest event occurred due to the Oldest Dryas warming, the largest event probably occurred at the end of the Younger Dryas (11,700 yBP), and the youngest of the documented events was purely of a Holocene age, with the highest landslide frequency being during the Atlantic temperature fluctuations (approximately 8200 yBP). The slope deformation occurred on a fault slope with a relative height of over 400 m and in tectonically weakened rocks. Sediments in the Most Basin were weakened from meltwater during rapid warming periods, which allowed mobilization of rockslide deposits and runout of up to 1000 m from the mountain foothills.

Keywords Landslide · Rock avalanche · Schmidt hammer · Paleogeomorphology · Krušné hory Mts

Introduction

The deposits of a large runout landslide[1] cover up to 778,000 m^2 on the south-east facing slopes of the Krušné Hory Mts. in the north-west part of the Czech Republic (Fig. 1). Many fossil slope deformations on the toe of the geomorphological expressive structural slopes of the Krušné Hory Mts. have already been described (Zmítko 1983; Špůrek 1974; Váně 1960), but the deformation under Mt. Jezeř (706 m a.s.l.) is quite exceptional due to its morphometric characteristics (Table 1).

The landslide was first described at the end of the 1950s; Váně (1960) mapped massive gneiss blocks deposited 1 km away from the mountain foothills. These blocks formed a morphologically significant hill named Šibeniční hůrka (285.9 m a.s.l.; on old mine map sheets named Galgenhübel) and was previously considered as an in situ gneiss outcrop, but analysis of old mine sheets and exploration drilling showed the existence of tertiary sediments of the Most Basin under the accumulation. A theory was formulated based on these findings, assuming that the gneiss blocks originate from the steep slopes of the nearby Mt. Jezeř (706 m a.s.l.) and the whole accumulation is a Plesitocene rock slide (Váně 1960). Additional studies of Špůrek (1974), Marek (1979), Rybář (1981), Zmítko (1983), and Růžičková et al. (1987) produced a substantial clarification of knowledge of the morphology and volume of this landslide (Table 1). In general, the accumulation around Šibeniční Hůrka is seen as a Pleistocene product of repeated rocksliding with a total volume of approximately 20 mil m^3 and an accumulation runout distance of up to 1 km from the foothills.

The development of surface mining associated with extraction of the entire overburden in the Most Basin led to excavation of this remarkable accumulation during the 1970s and 1980s (Fig. 2). Termination of this activity also led to a decline in interest in the issue of the landslide.

The aims of this present study are to summarize current knowledge of this large landslide and critically review the existing data and theories. However, the main aim was to acquire new data in order to estimate the age of the accumulation and clarify the movement mechanism. The study is based on a reconstruction of the whole landslide accumulation by digitizing military topographic maps of the Czech Republic from the 1950s and analyzing 216 boreholes drilled between 1941 and 2008. The entire slope deformation was analyzed in a GIS in order to reveal additional information about the area, volume, and structure, and a Schmidt hammer was used for dating the relative age of rocks in the head scarp and relicts of the accumulated blocks. The use of a Schmidt hammer for dating the relative age of the accumulated blocks was performed for instance in the case of the Huascaran rock avalanche (Klimeš et al. 2009) or on Svalbard (Hartvich et al. 2017).

Regional setting of the study site

The described landslide is situated in the foothills below the Mt. Jezeř (706 m) and Mt. Jánský vrch (736 m) and has created a significant hill Hůrka (286 m) in the area of the Most Basin. Both south-east-facing mountains are characterized by having slopes with a gradient of more than 30°. On the Mt. Jezeř, the gradient can reach more than 40°, with the steepest parts situated on numerous rock outcrops (Fig. 2). From east and west, the study site is delimited by the tectonically predisposed valleys of Šramnický brook and Vesnický brook.

The landslide deposits line the south-east foothills of the Krušné hory Mts. and run out into the Most Basin, which is a Neogene syn-rift basin between the České středohoří Mts. and Doupovské hory Mts. in the east and massif of the Krušné hory Mts. in the north-west (Fig. 1). The Krušné hory Mts. and the Most Basin present the main geological and geomorphological units (Balatka and Kalvoda 2006).

As a part of the Saxothuringian zone, the Krušné hory Mts. consist of crystalline complexes consolidated during the Cadomian orogeny and the mantle of Lower Paleozoic rocks weakly metamorphosed during Variscan metamorphism. The study site is made up of a

[1] The term landslide has been used here to refer to all types of mass wasting processes and their accumulations.

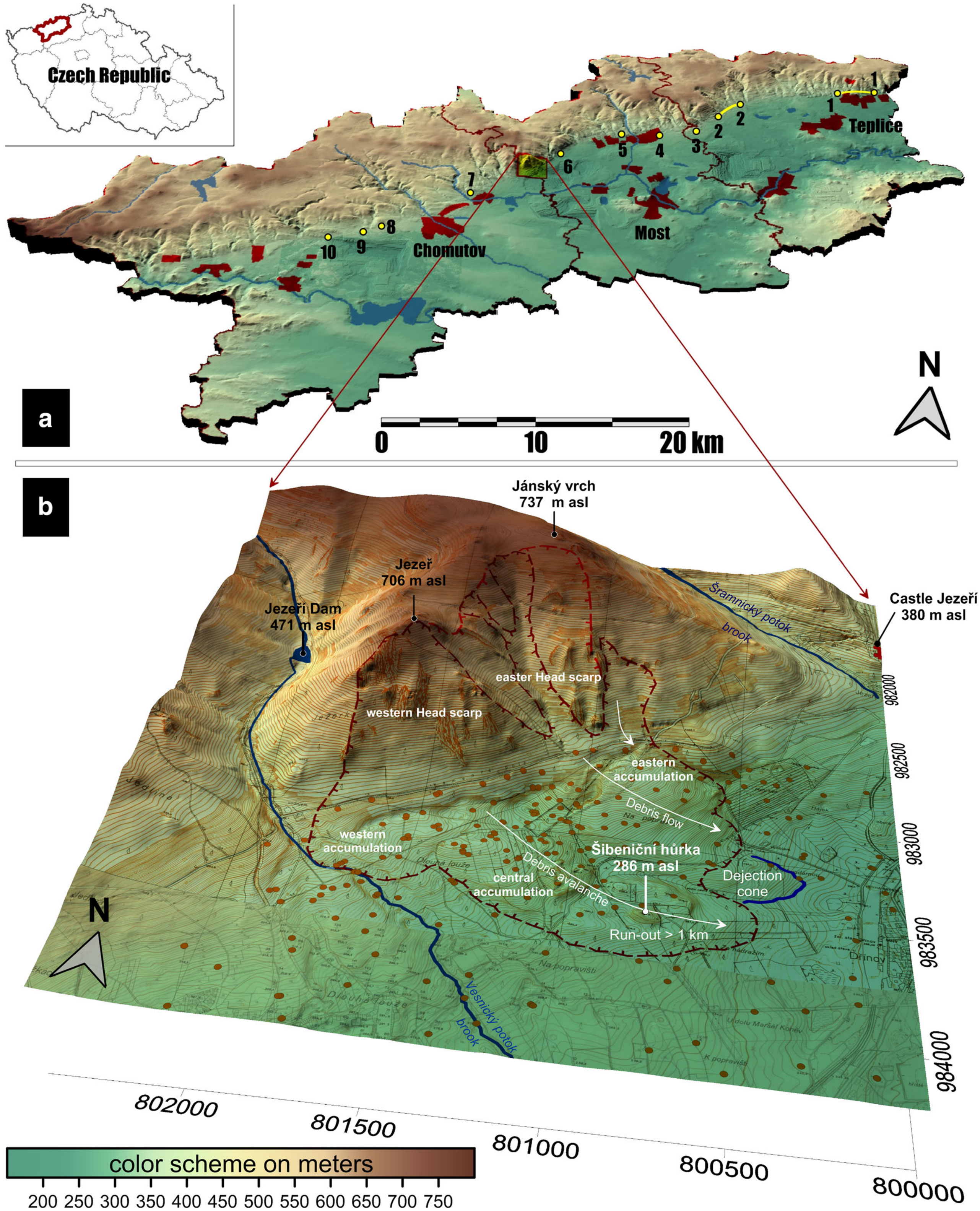

Fig. 1 Location of the study site and other slope failures on the south-facing slope of the Krušné Hory Mts. (according to: Zmítko 1983). *Legend*: 1—expected landslide area in Upper-Cretaceous-age sandy and marl sediments between Chlumec and Přítkov, 2—expected landslide area between Křižanov and Osek, 3—Salesius Hill formed by Tertiary-age sandstone and quartzite block fields (2–2.5 mil m^3), 4—plastic slope deformations in a coal seam near Litvínov, 5—area of gravitational slope deformations in crystalline rocks near Litvínov, 6—gravitational slope deformation (1 mil m^3) at the toe of Kapucín Mt., 7—block fields in the Bilina river valley, 8—Tertiary-age quartzite block fields on the slope of Hradiště Mt., 9—landslide (> 1 mil m^3) in Tertiary and Quaternary rocks at the edge of the Most Basin near Ahníkov, 10—landslide (0.5 mil m^3) in Tertiary-age tuffitic clays and colonized crystalline rocks near Prunéřov (**a**). A detailed 3-D view of the study site seen from south-DEM based on digitizing of military topographic maps of the Czech Republic from 1952 (**b**)

Table 1 The main landslide morphometric characteristics according to the following studies

	Váně (1960)	Špůrek (1974)	Marek (1979)	Rybář (1981)	Růžičková et al. (1987)[a]
Total volume	–	17–20 mil m^3	> 20 mil m^3	26.9 mil m^3	17–20 mil m^3
Total surface	–	635,000 m^2	–	–	635,000 m^2
Accumulation length	~ 1000 m	1000 and 500 m	1150 m	–	–
Accumulation width	~ 1200 m	350 and 300 m	~ 950 m	–	–
Max. thickness	70.2 m	70 m (ø 47 m)	up to 75 m	70 m	70 m (ø 47 m)
Altitude at crown	706 m a.s.l.	684 m a.s.l.	738.4 m a.s.l.	730 m a.s.l.	–
Classification	Rockslide	Two debris flows	Rockslide	Rockslide /rockfall	Rockfall
Type of movement	Sliding of a large gneiss block along bedding planes	First rocksliding along bedding planes changing into rolling	Gravitational spreading passing to rocksliding	–	Large block separation and its overtopping during the movement activity
Age	–	Pleistocene	Pleistocene	Pleistocene (Würm)	Pleistocene (stadial)

[a] Morphometrical parameters were taken from Váně (1960) in this study

portion of the Kateřinohorská klenba Vault (Kalvoda et al. 1990; Vilímek 1995)—a flat anticline structure oriented in a west-east direction. The core of this vault consists of orthogenesis and metagranites, which are adjacent to a series of crystalline shales. Longitudinal and transverse faults are applied with the prevailing directions of 60°, 296°, 332°, and 70° (Král 1968; Kopecký 1989), and the foliation surface is fan like with an inclination of 50° to 70° (Marek 1983).

The uplift of the Krušné hory Mts. in the Miocene–Pleistocene along the Krušnohorský Fault (Fig. 3) is expressed by the monoclonal folding of basin sediments near the edge of the mountains (Malkovský 1977). Also, as a result of uplift, the foothills are characterized by numerous slope failures from the Miocene, Pleistocene, and late Holocene (Zmítko 1983; Kalvoda 1995).

The piedmont area, including the Most Basin, has a graben structure (Váně 1985) and genetically belongs to the tectonic system of the Eger Graben (Domácí 1977). The basin sediments span the time interval from the Oligocene to Miocene. These sediments belong stratigraphically to the Paleogene-age Střezov Formation and dominantly to the Neogene-age Most Formation (Domácí 1977; Grygar and Mach 2013). In general, the crystalline basement is covered by various heterogeneous sediments of the lower Miocene clays, sands, and sandstones as well as denudational relict material of the Upper Cretaceous and weathered volcanic rocks—phonolite, basalt, and tuff. These Paleogene sediments pass into Miocene coal sedimentation indistinctly. The boundary between the coal seam and the Miocene clay complex is sharp, and these sediments comprise a group of clays and sandy-clays with variable carbonate occurrence. The average fill of this overlying complex can be up to approximately 175 m thick with a maximum thickness of 231 m (Malkovský 1985).

The Quaternary sediments predominately comprise coarse-grained gravels, sandy gravels, and clays with crystalline fragments. The thickness of sediments varies from 0.1 to 40 m (with an average of approximately 10 m) along the mountain foothills, and the rising thickness is associated with the alluvial fans or old fossil landslides (Váně 1960). Maximum thickness of Quaternary sediment deposits (70 m) was found directly in the study site—around the Hůrka elevation under Mt. Jezeř (Fig. 3).

Previous interpretations of the landslide

The elevation of Šibeniční hůrka and the surrounding hummocky terrain have attracted the attention of geologists and geomorphologist since the second half of the 1950s (Table 1). Both the character and size of the accumulation have puzzled geologists; the existence of a large gneiss block deep within the Most Basin was explained as a tectonic horst (Váně 1960). The development of open-cast mines has been associated with extensive mapping and survey of its forefields since 1950s. Based on these new findings, Váně (1960) outlined the assumption that the gneiss outcrops around Šibeniční hůrka are a large gneiss rock-slide-block. The accumulated material has a gneiss colluvium character, where rusty-brown coarse-grained weathered gneiss and whitish Kaolinized gneiss prevail in lower horizons. Váně (1960) also noticed several short recently buried galleries driven under Šibeniční hůrka from the north and the west. Several-meters-high, weathered, cracked but still coherent gneiss was described in one of these galleries as well as the fossil podzol soil profile.

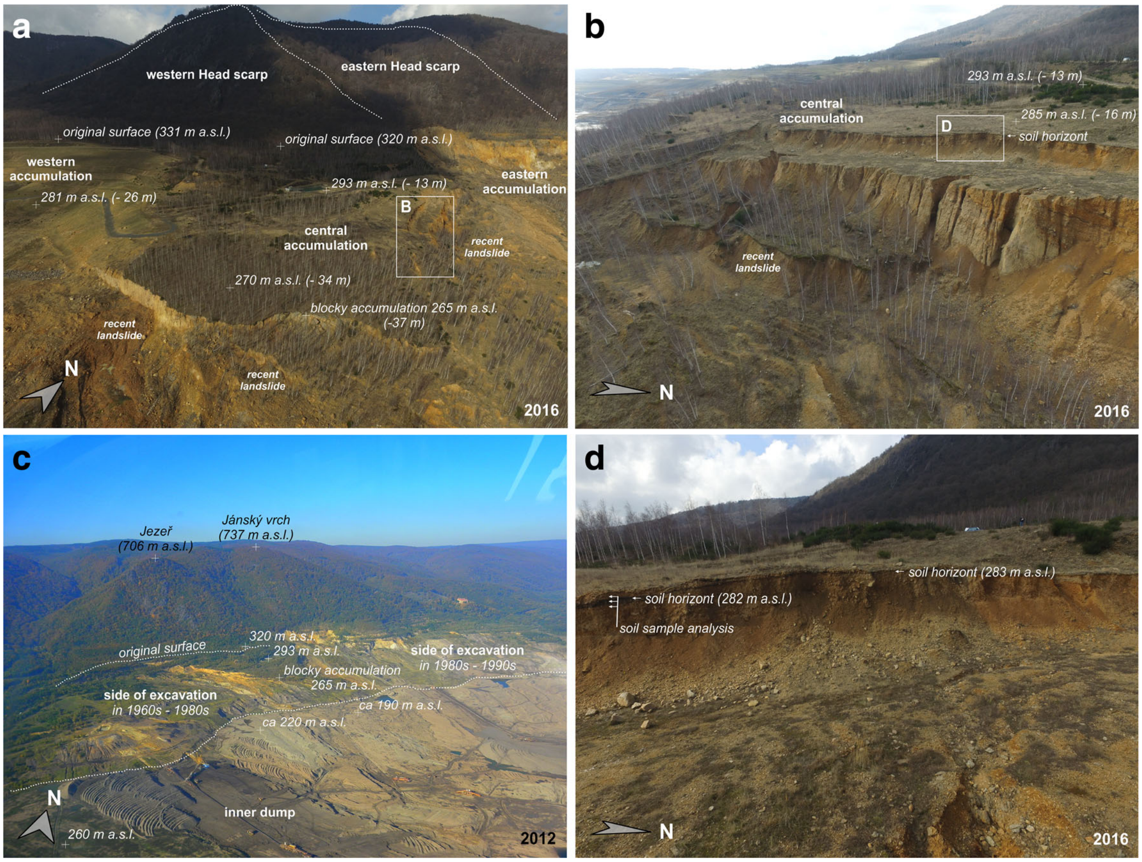

Fig. 2 An aerial overview of the landslide accumulation situated at the foot of the Jezerka (706 m a.s.l.) and Jánský vrch (737 m a.s.l.) and excavated due to open-cast mining in the second half of the twentieth century—the thickness of the excavated overburden is indicated in the parentheses (**a**, **c**). Dark and very sandy horizon visible in anthropogenic wall from 2013 (**b**, **d**). Photo: J. Burda, 2012 and 2016

A systematic geomorphological survey was conducted by Špůrek in the 1960s and provided a radical clarification of the morphology and structure of the landslide (Table 1). Špůrek (1974) described "Two debris flows originated by rock fall (or more precisely rockslide), of which the northern is probably older". A shallow valley separating both debris flows and the rounded shapes are evidence of the high absolute age of this phenomenon. He also describes the character of the accumulation, being of a clayey-sandy-rocky mixture with scattered and angular boulders exceeding 1 m^3 in size. Despite the fact that the blocks are coarse grained, micaceous, highly foliated, and weakly weathered, the matrix facies consists of strongly weathered, disintegrated, and kaolinized colluvium as a result of crushing during movement. Emphasis was placed on the rolling motion during movement, which enabled transport of the boulders up to a distance of 1 km from the foot of the mountains according to Špůrek (1974). The described landslide has a character of sudden and repeated movement along the predisposed cracks and foliation (50° to 70° in a southwest-northeast direction).

Although the studies by Marek (1979) and Rybář (1981) specify the extent of the head scarp boundary and volume of accumulation (Table 1), the question of emplacement mode and landslide classification of the given phenomenon has been addressed only marginally. The movement activity is assumed to have been triggered by seismic activity, most probably during the Pleistocene (Rybář in: Kalvoda et al. 1994). Rybář (1981) takes a closer look at large depression in the Quaternary basement, which is also evident from the cross-sections A-A' and B-B' (Fig. 4). According to his findings, the depression is of a pre-Quaternary age and cannot be explained by the compression of plastic clays due to landslide loading. Marek (1979) conceives this depression as an expression of a near-fault deformation.

Růžičková et al. (1987) provided a new perspective on this landslide. This study is also based on field research during the mining works in the 1980s. According to this study, large kaolinized gneiss blocks were situated mainly in the frontal part and near the base of the landslide accumulation, and also, the degree of gneiss weathering decreases with increasing elevation. Part of the described landslide accumulation had the character of colluvial sediments without signs of mass movements, and medium-grained sands were also identified in two boreholes. This study also described the Quaternary/Tertiary contact plane, which often has a slickenside character. Based on these facts, a new perspective on landslide evolution was submitted by Růžičková et al. (1987). Accumulation should be the result of large movement, when a large block was separated from the mountain slope and tilted over during this movement. Ideal conditions were during the stadial period, when the whole rock complex was temporarily reinforced by ground ice and subsequently deformed by landsliding. According to this theory, the sharply bounded accumulation basement is a former slope face and the upper accumulation parts are less-weathered rocks near the original sliding plane.

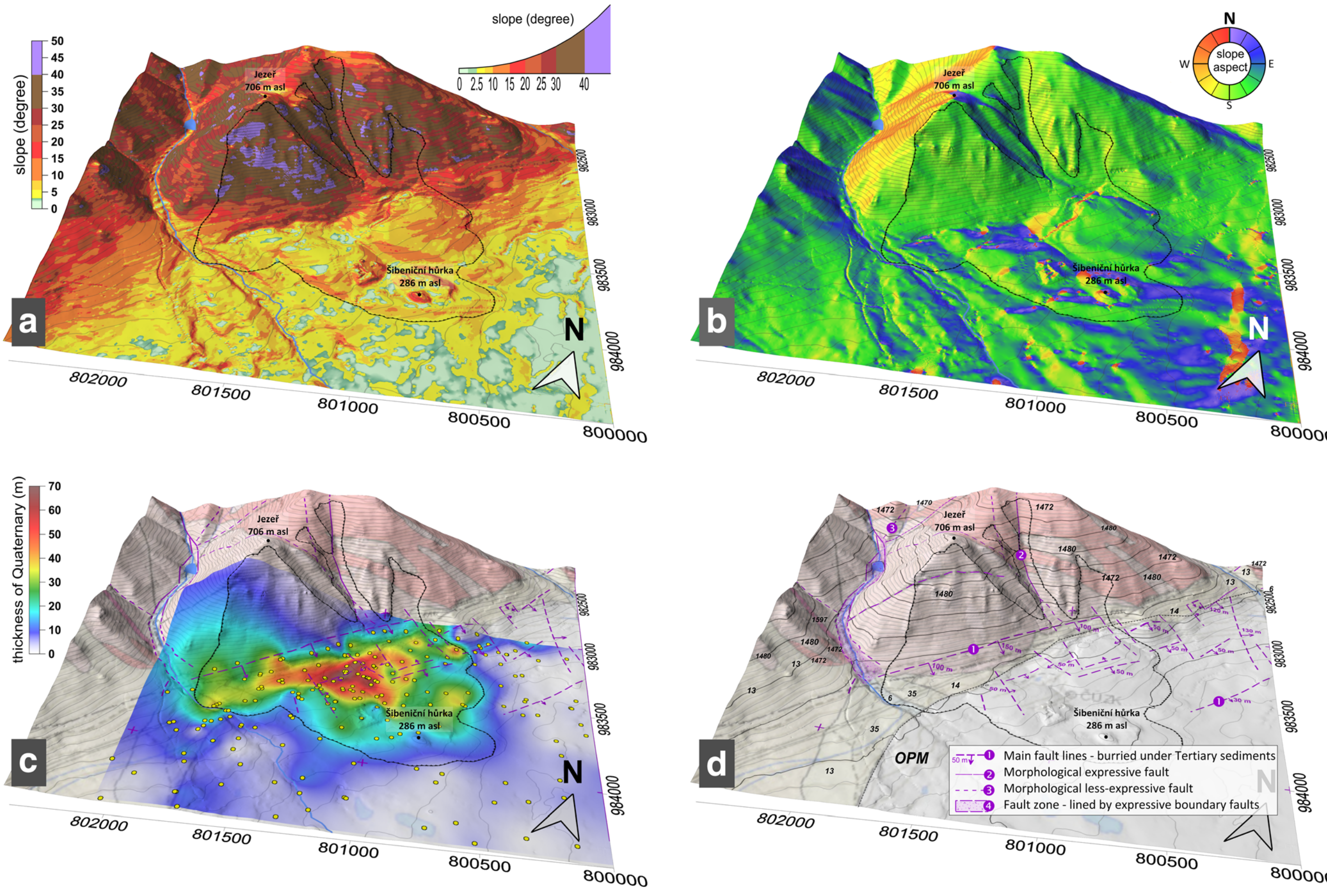

Fig. 3 3-D view of the south-slope steepness map (**a**) and slope aspect map (**b**). Geological settings of the study site—thickness of Quaternary sediments (**c**) and geological map: Quaternary deposits: 6—fluvial deposits, 13—stony/loamy sediment, 14—stony/blocky colluvium, 35—sands and gravels; Saxothuringikum: 1470—metagranite, 1472—coarse-grained eyed orthogneiss, 1480—leaf-orthogneiss, 1597—granite porphyry; OPM – open-pit mine in 2013 (**d**)

Material and methods

A review of the existing literature and engineering geological studies was the first step in the elaboration of this subsequent study. Secondly, military topographic maps of the Czech Republic from 1952 were geo-referenced, digitized, and used to reconstruct the original landscape from a pre-mining age. The crucial aspect of this research consisted of an analysis of 216 boreholes drilled between 1941 and 2008. During a detailed review of the borehole profiles, attention was paid to a proper assessment of the Quaternary base and description and analysis of the character and texture of the Quaternary deposits. The boundaries and thicknesses of other geologic units were also recorded.

Based on the abovementioned steps, a geological model, including the original 1950s surface, was compiled and analyzed in a GIS. This analysis enabled a better estimation of the landslide area and volume as well as the creation of longitudinal and transverse cross-sections and terrain modeling in particular the calculation of terrain slope and aspect (Fig. 3).

Field research

The surface hardness measuring is a method of dating the relative age of rocks (Goudie 2006). Stone blocks and rock walls in situ were tested for compressive strength using a Schmidt hammer type N, which works with an impact energy of 2.207 Nm. The device measures the rebound value (*R*) on a scale of 10–100 *R*. A table chart is attached to the hammer body, which shows the conversion between the *R* value and the compressive strength in a range of 10 to 70 N/mm^2. The test can be performed with the hammer in any angled position. The conversion table chart shows three correlation curves between the *R* value and the compressive strength.

The methodology according to Engel (2007) was used in this study, and areas of the rock with the same roughness (expected smooth slip surfaces) were selected. The measuring device was operated perpendicular to the rock surface and no impacts were made on the same point twice. Sampling sites were chosen via DEM analysis and verified during the fieldwork, while the criteria for choosing were accessibility and existence of morphological surfaces having character of potential shear planes. The distribution of sampling sites extends into the scarp area, the relict of the landslide accumulation as well as outside the landslide area. In the scarp area, only rock outcrops and rock walls in situ were chosen for the purposes of this study (Fig. 5). Boulders or rocks separated from the main crystalline massif were excluded during the fieldwork. The final mean *R* values were calculated after removing 20% of the most extreme values from each site (Engel 2007). Differences between *R* values were tested using Student's unpaired

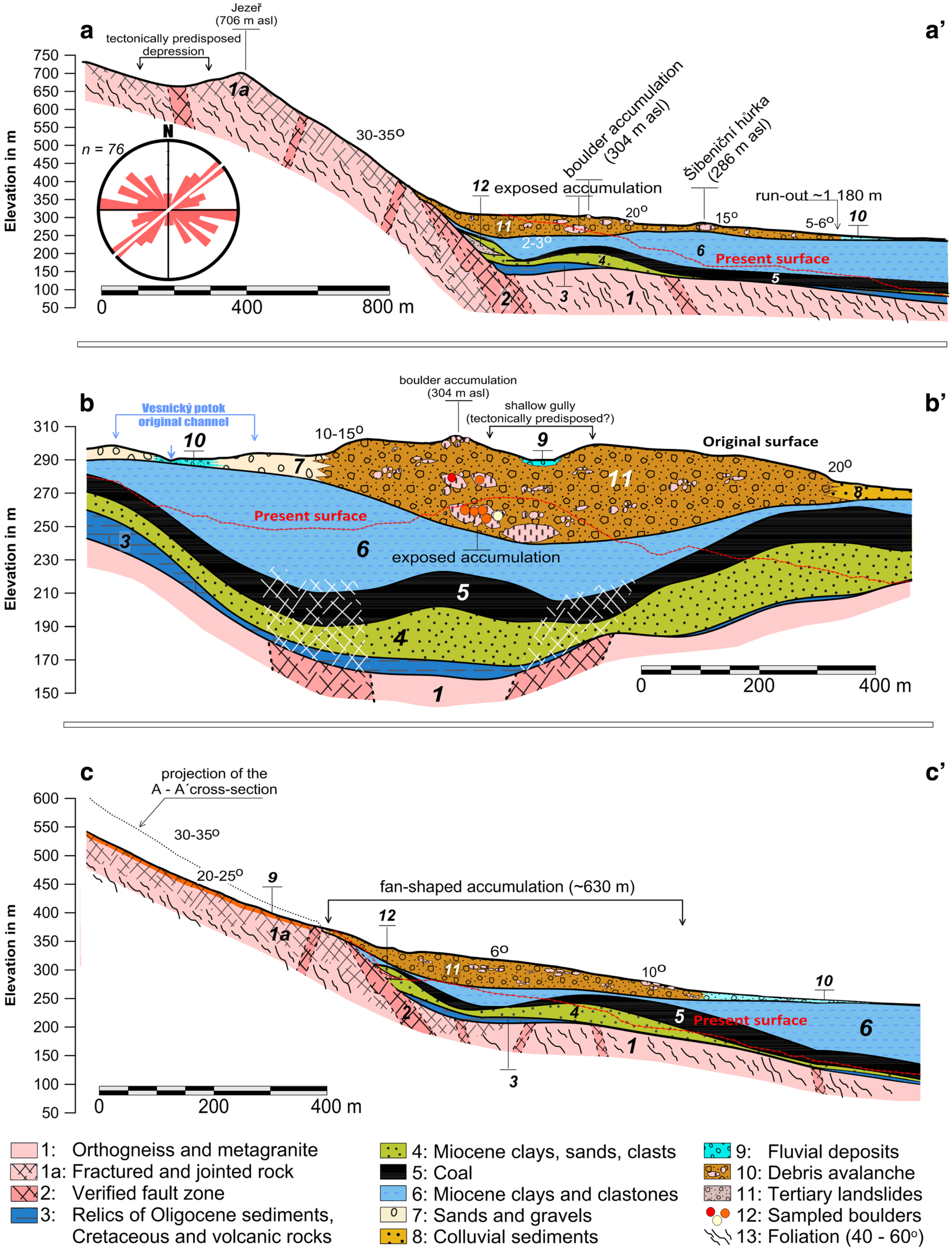

Fig. 4 Idealized cross-sections along the study site

two-sample *t* test comparing each other's results from scarp area, accumulation area, and outside the landslide area.

Mean *R* values were also used for an approximate age estimation, compared to an age-calibration curves from the Krkonoše Mts. (Czech Republic) described by Engel (2007) and Černá and Engel (2011), from Lake Superioir in Canada (Betts and Latta 2000), from Serra de Queixa in Spain (Sánchez et al. 2009), and from Jostedalsbreen-Sunnmore and Jotunheimen-Sognefjell in Norway (Shakesby et al. 2006). These time correlations were modified so that the young rocky outcrops, where we know the approximate age (about 100 years), match the respective *R* values.

Three soil samples from different soil horizons within the accumulation (Fig. 2d) were analyzed in the laboratory of the X-ray diffraction (XRD) in Brown Coal Research Institution j.s.c. Most. Diffraction analyses were carried out in diffractometer D 5000 Siemens according to the guideline IMP 009 of the Accredited Laboratory No. 1078.

XRD analysis is an analytical technique designed to provide more in-depth information about crystalline compounds, including identification and quantification of crystalline phases. In XRD analysis, a focused X-ray beam is shot at the sample (crystalline powder) at a specific angle of incidence. The X-rays deflect or "diffract" in various ways depending on the crystal structure (inter-atomic distances) of the sample. The locations (angles) and intensities of the diffracted X-rays are measured. Every compound has a unique diffraction pattern. In order to identify a substance, the diffraction pattern of the sample is compared to a library database of known patterns. In addition to identification of crystalline phases, the peak shapes and intensities collected during XRD analysis can be used to gather information about percent crystallinity and crystalline size.

Results

Landslide morphology, morphometry, structure

A simple geomorphological sketch map (Fig. 6), based on a 1950 DEM and modified using older geomorphic sketches (Špůrek 1974; Rybář 1981), presents the main features both in the accumulation zone as well as in the scarp area. In total, the accumulation part is 1180 m long, up to 1200 wide with relative relief of approximately 110 m. The total volume calculated in the GIS was set between 25.4 million m^3 and 27.4 million m^3. The deposits covered an area of 778,000 m^2, but the total contoured area of the slope deformations, including the scarp area, is 939,000 m^2 with a maximum length of 1650 m. The maximum thickness of the accumulated material is 72.1 m and was found in borehole KU 299 from 1985.

The head scarp area can be divided into two parts. The western part under Mt. Jezeř (706 m a.s.l.) has a morphologically expressive facetted character (fault slope), with numerous gneiss outcrops and rock walls on the surface. These rock outcrops in situ are concentrated at an elevation of 400 to 450 m a.s.l. up to the peak of Mt. Jezeř (Fig. 6) and this part of the slope is also the steepest—above 400 m a.s.l., the steepness rises from 20 to 25° to over 30° and in places over 40° (Fig. 3). The rock walls and outcrops are characterized by even steeper slopes—up to 90°. The eastern head scarp area, which is generally less morphologically expressive, has an

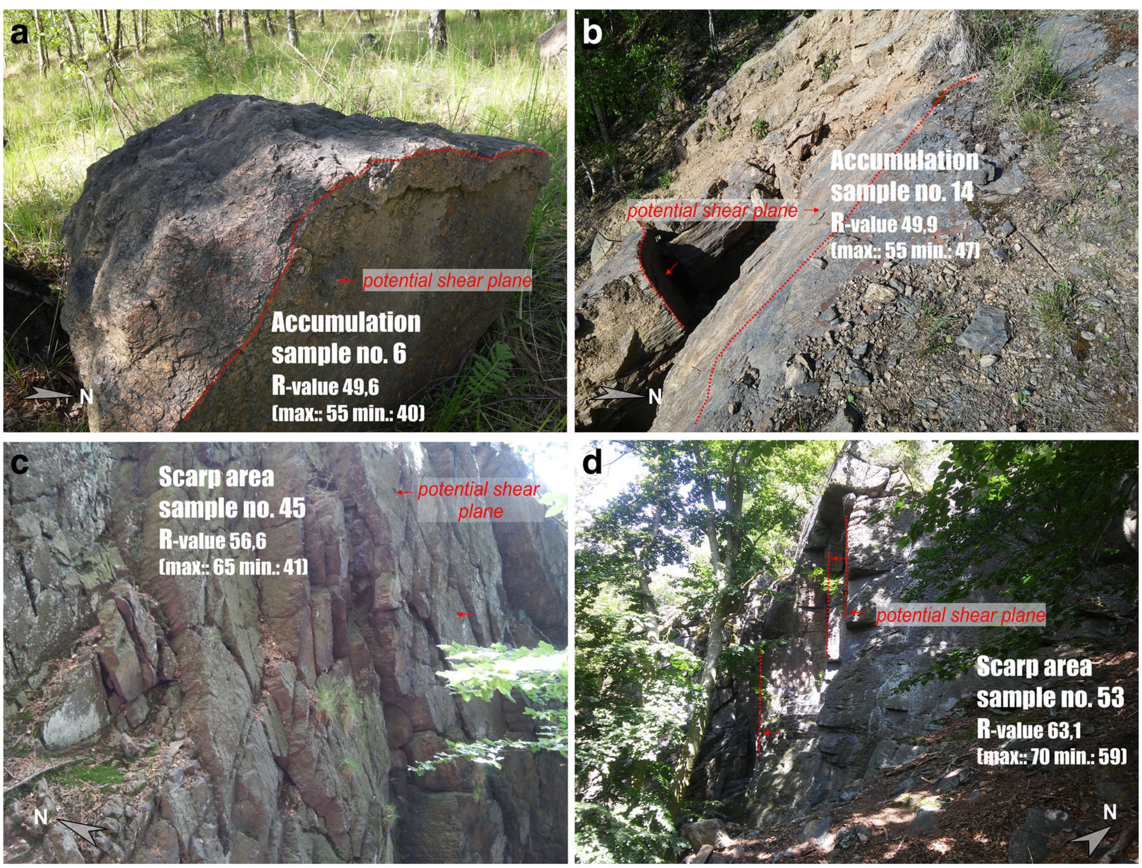

Fig. 5 Examples outcrop within scarp area and accumulation zone with attributed *R* values

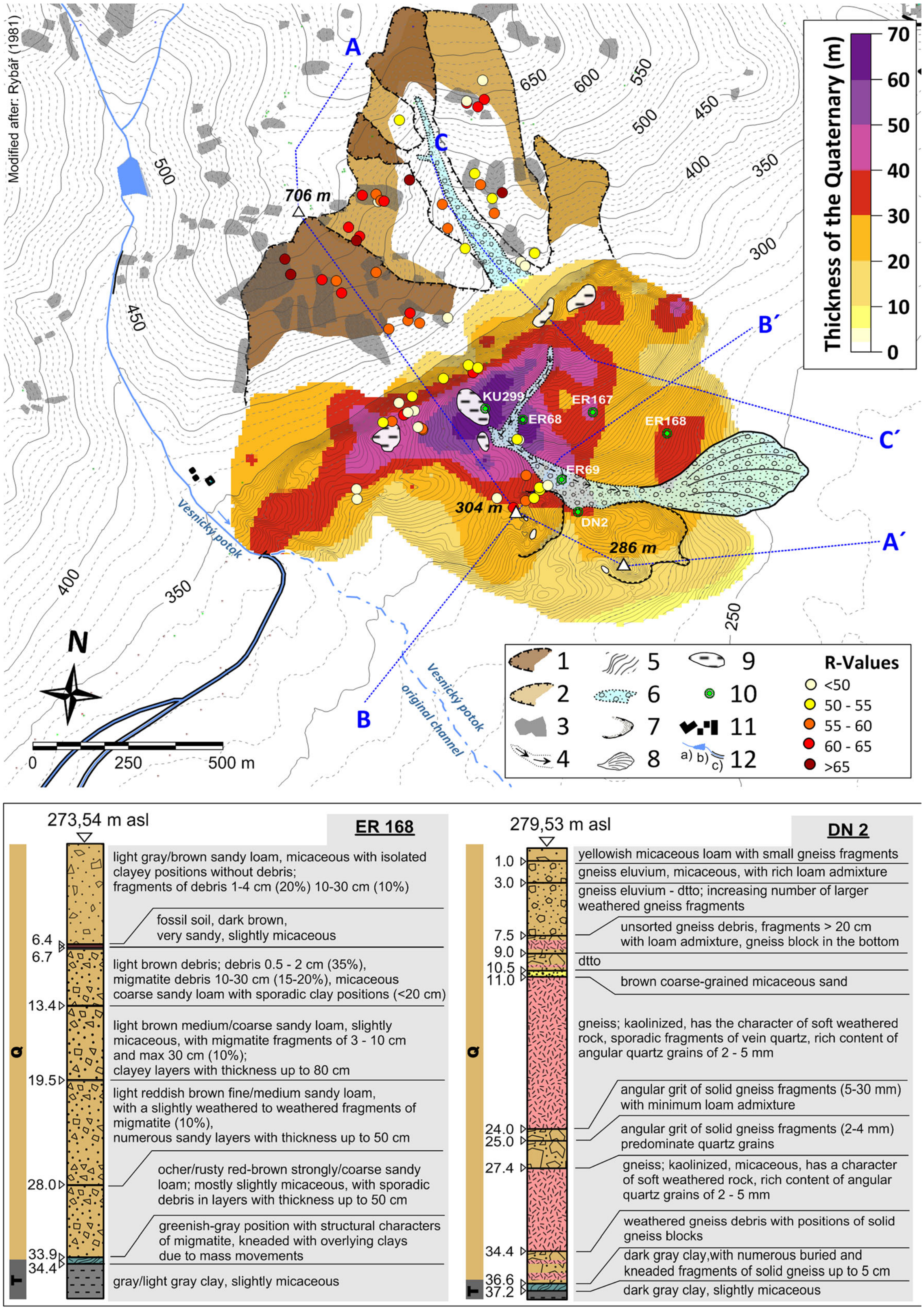

Fig. 6 *Top:* geomorphological sketch map of the landslide with marked positions of cross-sections. Legend: 1—scarp area with expressive margins; 2—scarp area without expressive margins according to Rybář 1981; 3—rock outcrops, small ridges and rock groups; 4—gullies with occasional streams; 5—the main deposit area (contour interval 1 m); 6—fluvial sediments; 7—expressive accumulation toes with hummocky surface; 8—proluvial cone; 9—shallow colluvial depression; 10—boreholes mentioned in the text; 11—buildings and houses; 12a—stream with natural channel, b—dam, c—artificial stream channel. Bottom: geological description of ER 168 and DN 2 borehole profiles

amphitheatrical shape which surrounds an expressive erosion gully in the middle. This gully is 550 m long, 50–120 m wide, and in the upper part splits in two particular scarp areas, which are morphologically more distinct than the rest of the eastern scarp area. This large gully is predisposed tectonically (Rybář 1981) and is filled by fluvial sediments at the bottom. The upper edge of this source area reaches up to 730 m a.s.l. Some rock outcrops are located around the central gully, but in general, rock walls and rock outcrops are less common comparing to the western source area.

Morphologically, the whole landslide accumulation can be divided in three main parts (Fig. 1): western and central part—both directly below the western scarp area of Mt. Jezeř and the western part extends up to the valley of Vesnický brook. The central and eastern accumulation parts are separated from each other by a shallow broad valley.

The surface of the western accumulation part is geomorphologically indistinct without expressive accumulation forms. The maximum Quaternary sediment thickness reaches 38.5 m in the flat valley of Vesnický brook (Fig. 6). This landslide accumulation also diverted the flow of Vesnický brook and resulted in a small meander. The deposits have a character of angular boulder gneiss debris (fragments of size 100–300 mm up to 20%) with a several-meter-thick layer of loamy sand in the Quaternary basement. Sandy layers represent the material of the original alluvial fan, which was later buried due to the mass movement deposits. Recently, stream erosion cut across these deposits and formed a new flat valley with steep slopes and was filled with alluvial sediments (Fig. 6).

The central part of the landslide accumulation was excavated largely due to the coal mining in the 1970s and 1980s. From the 1950 DEM, it is obvious that the central part is clearly demarcated by 10–15° sharp and approximately 10 m high linear side limits from the west and by a broad depression from the east. The accumulation has a runout character with an irregular hummocky surface and two expressive elevations (see Fig. 4 and Fig. 6: Šibeniční hůrka 286 m a.s.l. and a nameless boulder at an elevation of 304 m a.s.l.). These elevations were formed by one or more large blocks of solid coarse-grained gneiss up to thousands of m^3 (Špůrek 1974; Rybář 1981). Both elevations represent the most recent runout phases and are characterized by a 15–30° step south-east-facing slope with small dry depressions on top. The length of the Šibeniční hůrka runout is 950–1000 m (with a thickness of the colluvial deposits of 27 m), but the maximum length, from the mountain foothills to the older indistinct accumulation toe at approximately 252 m a.s.l., reaches 1180 m. The thickness of the landslide deposits reaches up to 72.1 m in KU 299 (Fig. 6). The area with Quaternary sediments' thickness exceeding 40 m is linked to a depression, which is evident in the pre-Quaternary basement—in the Tertiary sediments and partly in the crystalline fundament (Fig. 4). This depression is obvious from both longitudinal and transverse cross-sections A-A' and B-B' and it is predisposed tectonically according to Fig. 3, which was also assumed by Marek (1979). From cross-section A-A', it is obvious the Quaternary-Tertiary interface is almost horizontal, but between mountain foothill and the nameless boulder elevation (304 m) even rising slightly at an angle 2–3°.

The character of landslide deposits was described well in borehole DN 2 from 1958 (Quaternary sediments thickness of 36.6 m). In the upper 7.5 m, the material has the character of gneiss colluvium with a rich loam admixture and an increasing number of larger weathered gneiss fragments. Kaolinized and weathered soft gneiss with angular fragments or blocks of solid gneiss follow in the next 29.5 m and pass into a 0.6-m-thick layer of dark gray clay, solid gneiss fragments, and soft weathered gneiss debris, which are kneaded together. A similar character of landslide deposits was described in numerous other boreholes in this part of the landslide. The matrix facies consist of unsorted and strongly weathered gneiss debris, often colonized and with a rich loam admixture texturally interspersed with angular gneiss fragments to 30 mm (up to 30%). The block facies include large solid or slightly weathered blocks of coarse-grained gneiss or migmatite from 20 cm to boulders in size of meters. The contact of the Quaternary landslide material and the Tertiary layers comprises of dark gray clay, with numerous buried and kneaded fragments of solid gneiss up to 5 cm. A similar geological profile, including solid gneiss blocks, was found in many boreholes within the central accumulation (e.g., ER 68 and ER 69).

The majority of this accumulation has been excavated in the past (Fig. 2), but due to the mining, recent landslides, and current stabilization earthworks, some new boulders and gneiss blocks have been exposed. A large gneiss block is exposed approximately 37–42 m below the former nameless boulder elevation (304 m). The crown is at an elevation of 262 to 267 m a.s.l. and the visible part is 60 m wide and 5–9 m high. During the field mapping, it was not possible to determine whether it is a large single block or several blocks placed in one sedimentary layer. Nevertheless, this block(s) is comprised of angular solid gneiss and is located approximately 10 m above the Quaternary basement. Similar large solid gneiss blocks were described in the nearby borehole ER 69 (Fig. 6); these blocks were placed in three horizons: the first 274.8–273.8 m a.s.l., second 257.8–254.8 m a.s.l., and third 250.8–240.8 m a.s.l. The thickness varied between 1 and 10 m, and these gneiss accumulations were separated by layers of gneiss gravel with a sandy-loam admixture.

The central and eastern parts of the landslide accumulations were morphologically separated by a 120–130-m wide valley modified by occasional water streams and elongated in a south-east direction. The length exceeds 500 m with an average depth of approximately 10 m. The valley bottom is filled by unsorted clasts (Špůrek 1974) and passes into a less morphologically distinct, rather supposed, debris cone. The valley axis follows the depression in the Quaternary and pre-Quaternary basement; hence, the valley is linked to the area with the highest landslide deposit thickness (Fig. 4).

The eastern landslide accumulation was excavated almost completely in the past up to the crystalline rocks of the Krušné hory Mts. This fan-shaped accumulation was up to 630 m long with a surface inclination of 10–15° in forehead part and 5–10° at the crown (Fig. 4). The depression, which is evident in the pre-Quaternary basement—in Tertiary sediments and partly in crystalline basement, is obviously also in cross-section C-C'. The character of landslide deposits is slightly different from the landslide accumulation in the central part, which is evident from geological borehole ER 168. Large blocks of weathered gneiss are missing; accumulation has the character of slightly gray or brown sandy loam with relatively small angular fragments (up to 50 cm) of gneiss debris or migmatite (proportionally 10–20%). Dark brown, very sandy, and slightly micaceous fossil soil was described in the depth of 6.4 m (267 m a.s.l). Similar dark and very sandy horizons are visible on the anthropogenic walls (at 279 and 269 m a.s.l.) from 2013 situated 290 m to the west of ER 168 (Fig. 6). Like in DN2 borehole, the contact of Quaternary landslide material and lower Tertiary layers comprises a dark gray clay, with numerous buried fragments of solid gneiss kneaded due to mass movements. A similar geological profile, including a layer with kneaded clays and gneiss debris, was described in borehole ER 167 and in several others.

Schmidt hammer testing

Rock hardness measurements were performed on 72 sampling sites suitable for the Schmidt hammer test, mainly on the youngest morphological surfaces having character of potential shear planes. For comparison, 12 sampling sites were chosen outside the landslide area. Differences of *R* values from all three sampling sites were statistically significant with $p < 0.05$.The result of *t* test showed statistically very significant difference ($p = 0.0008$) between both samples from scrap area and outside the landslide area. *R* values from the accumulation zone and the scarp area showed significant difference too ($p = 0.0073$). Statistically less significant difference was found within the data from accumulation area and outside the landslide area ($p = 0.0329$).

The compressive strength *R* values for the head scarp are in the range of 43.5 to 69.9, with a mean value of 57.8 and mean standard deviation of 4.0 (Fig. 7). In the accumulation zone, *R* values are in the range of 44.5 to 68.7, the mean value is 53.9, and the mean standard deviation is 4.2. These values represent rocks with different levels of strength/weathering (modified after Selby 1980), from very high strength rocks (> 65) to rocks with lower strength (< 50).

The rocks of the head scarp area have significantly higher *R* values than the deposits in the accumulation. From the eight highest values, with an *R* value of over 65, only two were situated on boulders in the accumulation zone and over 70% of the sampling sites in the landslide accumulation zone are in the lower half of the dataset (Fig. 7).

Rock outcrops in the western head scarp area are characterized by higher *R* values (43.5–69.9; avg. 59.2), compared to the eastern part of the head scarp area (47.0–65.1; avg. 54.8). In the western part, the slopes are steep (more than 30° and up to 90° on the exposed rock walls) with a higher inclination than the eastern part of the scrap area; rock outcrops are also larger and more common here (Fig. 4). Sampling sites with different *R* values are distributed in both the western and eastern scarp areas. High strength rocks (*R* value > 60) are placed in the upper site of the western part, while the middle of the slope is characterized by *R* values of between 50 and 60, and two sampling sites with medium and low strength are situated lower on the slope. This elevation dependence is not conclusive in the eastern part; on the contrary, the rock strength is distributed irregularly throughout slope with a slight decreasing trend in rock strength towards the east.

The terrain of the original landslide accumulation was more modified due to open-cast mining; these excavations removed the southern rim of the landslide accumulation and also its surface layers. However, older debris material, including large gneiss blocks and boulders, were exposed due to these excavations. Five sampling sites were tested on a large blocky accumulation (crown at 262–267 m a.s.l.) under the former nameless elevation (304 m a.s.l.), and the *R* values span from 49.6 to 55.4. Another 24 smaller exposed gneiss blocks or boulders were tested in the rest of the accumulation zone, whereby the *R* values varied from 44.9 to 66.0. Different *R* values represent different landslide events placed rather randomly within the accumulation. The lowest *R* values (< 50) were detected rather closer to the mountain foot, and a cluster of the most similar *R* values (mean standard deviation 1.5) concentrated to one place is the exposed blocky accumulation mentioned above. The highest *R* values (> 60) were found on medium-size boulders, one of which is located on the current surface near the blocky accumulation and two are close to the mountain foot.

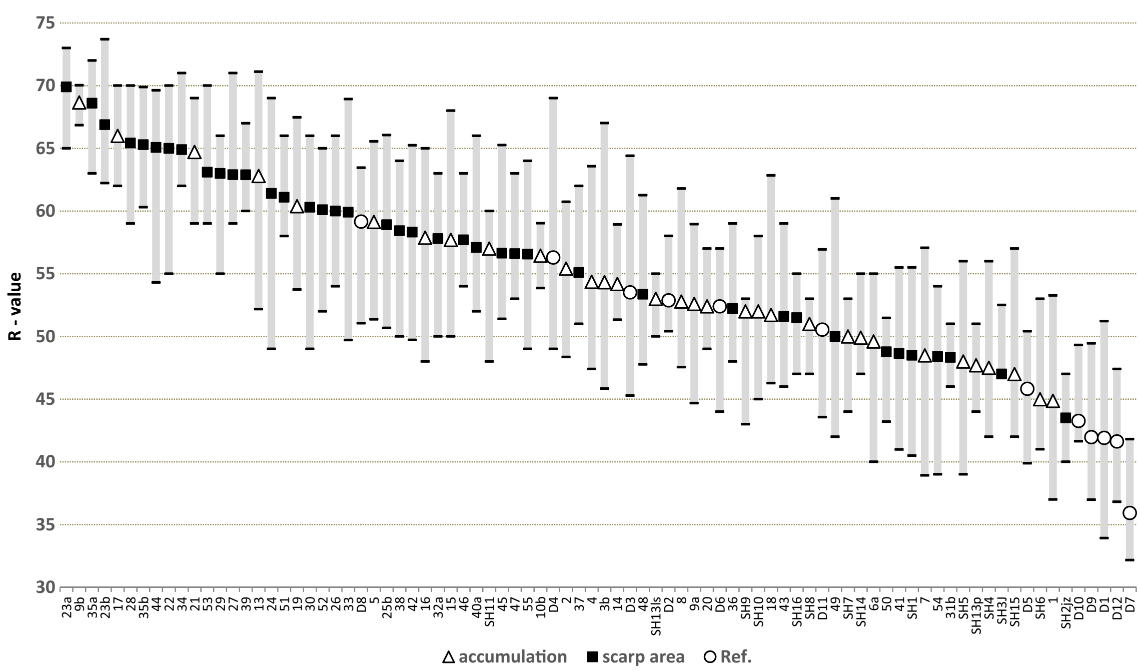

Fig. 7 Schmidt hammer *R* values—in the scarp area and the accumulation zone

X-ray diffraction of soil samples

We took one sample from expected soil horizon, one sample from underlying horizon, and one sample from overlying horizon. The mineralogical content of these samples is very similar. The main identified minerals are quartz d: 4.26(6), 3.34(10), 1.82(5), 2.24(4), 1.55(4), 1.08(4) Å; albite d: 3.19(10), 3.20(4), 4.00(5) Å; kaolinite d: 7.16(10), 2.21(5), 4.47/(4), 3.58(3), 1.66(3) Å; biotite d: 10.08(10), 2.94(5), 2.45(4), 1.55(4) Å; and muscovite d: 9.98(10), 4.49(6), 3.33(4), 2.56(4), 2.45(3) Å. Trace admixture consists of kaolinite, illite, and montmorillonite.

Mineralogy of analyzed samples is very similar, but the sample from expected soil horizon includes the admixture of amorphous mass. This amorphous mass is probably organic. From the point of view of XRD, this sample is probably fossil soil because of this amorphous mass. Result of XRD analysis is shown in Fig. 8.

All samples' contents have the same characteristic minerals—the quartz, the feldspar, and the mica (primarily muscovite). The admixture contains clay minerals. Expected soil horizon includes the admixture of organic mass. The mineralogical content indicates the same mineralogical origin of three analyzed horizons—the gneiss of the Krušné Hory Mts. crystalline complex. The rare admixture of clay minerals suggests the existence of weathering processes. It is not possible to differentiate the origin of organic mass in the expected soil horizon (coal or humus) only according to XRD, but the content of Cox according to chemical analysis probably indicates the existence of soil horizon. Stratigraphic break before sedimentation of underlying stratum probably enables the genesis and the development of this soil horizon.

Landslide classification

Based on the existing knowledge, we conclude that the slope deformation (or its western part) is a rockslide-rock avalanche, whereby the presence of water was crucial and allowed the transport of the material up to 1200 m. The water could be injected into the mobilized matrix from stiff, fissured, water-saturated Miocene sediments at the foot of the mountains or earlier due to snow or permafrost melting. If we consider the approximate age determined based on the Schmidt hammer testing, the largest movements probably occurred at the end of the Pleistocene. During this age, the large Lake Komořany formed in the Most Basin immediately below the slopes of the Mt. Jezeř and Mt. Jánský vrch (Jankovská 1987). Its maximum surface area is estimated to be 52–57 km^2, at a length of 13 km and a width of 9.5 km (Schlesinger 1871; Zapletal 1954). Sediments of this lake were found at 230 m a.s.l. (Jankovská 1983),

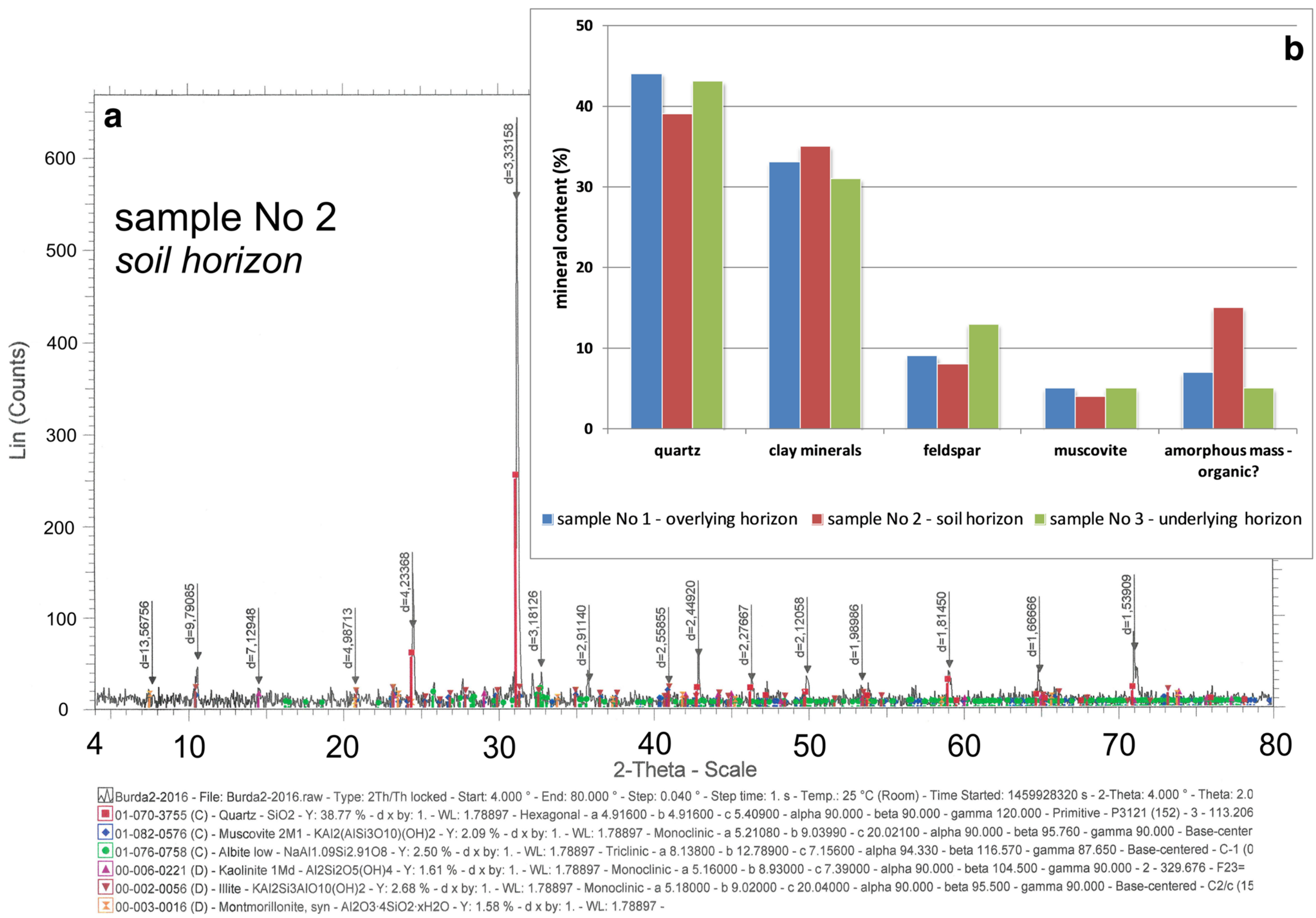

Fig. 8 Result of XRD analysis—sample No 2 (**a**). Content of minerals in samples No 1: overlying horizon, No 2: soil horizon and No 1: underlying horizon. The variety in the mineral components of all samples is the difference in the proportion of amorphous mass, which we assume is made up of organic. Therefore, we assume it is a poorly developed soil horizon and thus these horizons represent sediment of various ages. Content of minerals in every sample was determined only indicative according to area and altitude of main peaks of each mineral (**b**)

whereas the rock avalanche sediments were at a higher gradient (Fig. 4); we conclude that the accumulation did not reach the lake. The groundwater level in the area of the lake was near the surface and because the average annual temperature of Most Basin was 4 °C in the Younger Dryas (Jankovská 1987), regelation processes were also intensive (to a depth of up to several tens of meters; Marek 1983). In the mountains, the average annual temperature was 0° C, slopes were without tree vegetation, and only covered by tundra vegetation (Jankovská 1987). According to the expected scenario, a rockslide-rock avalanche could occur as a result of warming at the end of the stadial, as a result of rising temperatures melting the snow cover and permafrost. Rising groundwater levels and filling of the tectonic cracks by melting water could also be one of the possible triggering factors.

Discussion

Based on the Schmidt hammer results, we can indeed conclude that mass movements were repeated and accumulation is a result of several mass movement events, which corresponds to the conclusions of Rybář (1981). The *R* values span from 43.5 to 69.9, both in scarp area and the accumulation zone, and it can be concluded that the sampling sites with the *R* values represent rocks with high or very high strength, therefore, less-weathered and solid rocks or as a result of fracturing and changes in structural properties during the movement. Rock outcrops and boulders with *R* values < 60 or < 50 represent older and therefore more weathered landslide events. In general, the eastern scarp area seems to be older, which is also in accordance with the conclusions of Špůrek (1974), despite only younger and less-weathered rock outcrops (*R* value > 60) being found in the western scarp area. On the other hand, the range of *R* values in the accumulation zone is from 44.9 to 66, which may indicate deposits of several mass movement generations, many of which seem to be older than the rock outcrops on the present slope face of the western scarp area. We assume that this is due to slope rejuvenation by younger mass movement activity, whose accumulation was largely excavated during the mining in the 1980s, which exposed older accumulation generations. We also assume rejuvenation of the eastern scarp area due to local mass movement, but because the eastern accumulation was completely excavated, it is impossible to compare the results from eastern scarp to any results from the accumulation part.

Taking into consideration the morphology and measured *R* values, it is obvious that the western scarp area was rejuvenated by mass movements even later (after event 3) but the corresponding sediments do not exist. Therefore, we assume that the mass movements, although smaller in scale, continued almost until recent time (mainly in the western scarp area). The oldest event cannot be determined generally either, because the majority of the accumulation was excavated and the scarp areas were most probably rejuvenated by younger events. The determination of age must be taken with a certain reserve, as it is associated with the inaccuracy of the Schmidt hammer method—individual measurements have a large variance within each sampling point. Moreover, the Schmidt hammer method is a method of relative dating; the correlation equation we used was calibrated in the Krkonoše Mts., which is a part of the Bohemian massif and is geographically and geo-morphologically the most convenient of the available correlations; nevertheless, its use could be associated with errors, which are determined by regional geological differences of both sites.

According to Copons et al. (2009), prediction of rockfall transport distance is an indispensable activity in rockfall susceptibility and hazard and risk assessment. This is why we first ascertain the volume of the landslide and other morphometric parameters. Nevertheless, the character of the environment is very important for the runout distance. Okada and Uchida (2014) showed using a physically based model the difference between water-saturated experiments and those under dry conditions. The final deposition was 10% larger in a water-saturated environment.

Even though the structure of the accumulation was described well in previous studies (Table 1), its movement mechanism and landslide classifications were described very vaguely and are often untrustworthy. In general, there is a consensus that the gneiss block was separated along a tectonically predisposed plane or bedding planes and then the rocksliding occurred. The accumulation toe reached up to 1200 m from the mountain foothills due to the rolling motion (Špůrek 1974). Similar events were described by Strom and Abdrakhmatov (2016) from the Central Thien Shan in terms of a long distance runout. A different movement mechanism was described by Růžičková et al. (1987), according to whom the movement had a character of large toppling, when the whole slope face tilted over and was temporarily reinforced by soil ice during this process.

This hypothesis is not considered to be realistic, because firstly toppling is more typical for almost vertical rock walls with bedding planes parallel to the rock face (Němčok et al. 1972), and secondly, the function of soil ice as the binder that holds together the entire toppled block seems to us to be extremely unlikely. We believe that the tensile strength of soil ice is not sufficient (lower than in the gneiss) to withstand the tensile stresses imposed during the course of such a type of movement.

Based on today's knowledge, studied landslide can be described as a rockslide-rock avalanche type. However, despite the considerable energy of transported masses, from a kinematic point of view, it is unlikely that simple rolling moving mechanism described by Špůrek (1974) would transport blocky gneiss debris for a distance of up to 1200 m, which is almost four times the length of the head scarp area. Given the high friction angle of the blocky debris (ϕ approximately 30°), rockfalls, toppling, or rockslides are often accompanied by large talus cones at the foot of the slopes in places where the slope decreases. Stoffel (2005) argues that the movement slowdown and sliding material accumulation occur in areas where the gradient of the relief decreases below 30°. The gradient of the head scarp area is 30–35°; in this case, the material was accumulated in the planar relief of the Most Basin. The contact between the Miocene clays and debris accumulation is rising at an angle of 1–2° directly at the foot of the hill. From the foregoing, we conclude that another movement mechanism was applied, which allowed the transport of such an amount of blocky debris up to a distance of 1200 m. Transport of substantial volumes (tens of millions of m^3) of coarse unsorted material for several kilometers is typical for debris or rock avalanches, which often represent the largest regional slope deformations. When the matrix, consisting of various fractions from gravel to boulders of up to tens of meters, is sufficiently saturated by water, the material run-off can be up to several kilometers from the head scarp area (Goudie 2004). The water, allowing this run-off-movement, is typically injected to the matrix from sediments deposited under the head scarp area as a result of a sudden load by the rock mass (Crandell 1989).

Geological boreholes and previous work (Růžičková et al. 1987) demonstrate the presence of a colonized gneiss block even in the accumulation area. The colonized gneiss, as a material in the tectonic breccias, was also discovered in the faults on the surrounding slopes. Within these faults, the colonized gneiss is always impermeable (Marek 1983); this results in an increase in pore pressure, which may have triggered large rock sliding on a predisposed surface (Sartori et al. 2003). In the basin, the sudden impact of several millions m^3 of rockslide material could cause compression of stiff-fissured soft Miocene clays and due to the high level of the groundwater as well as its boiling. This incoherent and saturated material was mixed with a rockslide matrix and could have the function of a mobile layer, allowing run-off of the original rockslide material (as was already suggested by Hurník 1986). This fact is proven by the position of a sharp layer of kneaded clays identified on the base of the accumulation (Marek 1979; Fig. 6—borehole DN2). This rockslide-rock avalanche scenario seems to us to be very likely in the central accumulation.

In the eastern accumulation, we assume that it is actually the product of repeated debris flow (or at least the latest phases). It is supported by the scarp area character (dominated by large erosion gully), and morphological character of the accumulation, which was fan shaped with a gentle slope (Fig. 6). The gneiss blocks described in the boreholes were also smaller and less frequent compared to the central accumulation part (see Fig. 6—bottom). A sharp layer of kneaded clay was found in boreholes ER 168 and ER 167, which may suggest older sediments were transported up to 650 m from the mountain foothills in the form of a rock avalanche and were subsequently overlaid by a younger debris flow deposit. The western accumulation part has a more colluvial character, and the boulders and blocks are less frequent, less rounded, and smaller (Špůrek 1974). Therefore, we assume that the extent of the rock sliding was less, more solitary, and with a possible rolling character.

The colluvial depressions, erosion gully, deformed soil, and debris horizons within the accumulation may be the result of initial sedimentation or sudden mass movements of continuing tectonic processes in the Holocene.

We also attempted to estimate the approximate age of the sampling sites using age-calibration curve assembled by Engel (2007). This regression equation was chosen from several studies (Betts and Latta 2000; Shakesby et al. 2006; Sánchez et al. 2009), because it is based on dating in the Krknoše Mts., which is also part of the Bohemian Massif and has some geomorphological and climatic similarities to the Krušné hory Mts. Rebound values are influenced by strength of the intact rock, state of rock weathering, rock jointing characteristics (spacing of rock joints, joint width, joint continuity, joint infilling, and orientation etc.), and also water seepage from the rock face. Not all these parameters are of equal importance but each of these factors gives a rating value according to their perceived influence on stability of the rock slope (Goudie 2004). Due to the inaccuracy of the Schmidt hammer method and the variability of measured values (Viles et al. 2011; Goudie 2006), we hypothesized that a single event can have results ranging from hundreds to several thousand years. Following this approach, it was found that the tested rock outcrops, blocks, and boulders are from a recent age up to approximately 15,200 yBP (Fig. 9) and three main events (or a period of several smaller events in quick succession) were identified—evidence was found both in the scarp area and accumulation area. Because most of the accumulation was removed, it is possible that the blocks, older than those we found during the fieldwork, were also excavated. It

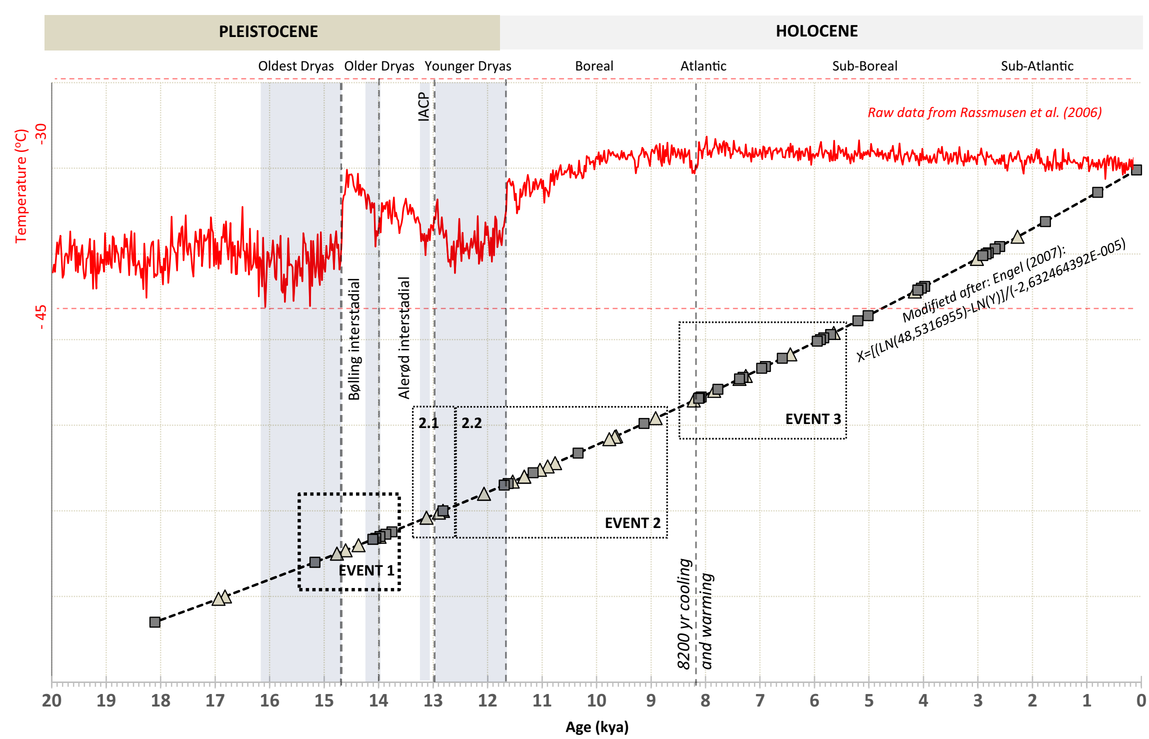

Fig. 9 Rough age determination of analyzed rock faces by age-calibration by Engel (2007) showing the postulated events and late glacial climatic trends as recorded in the NGRIP Greenland ice core (Rasmussen et al. 2006)

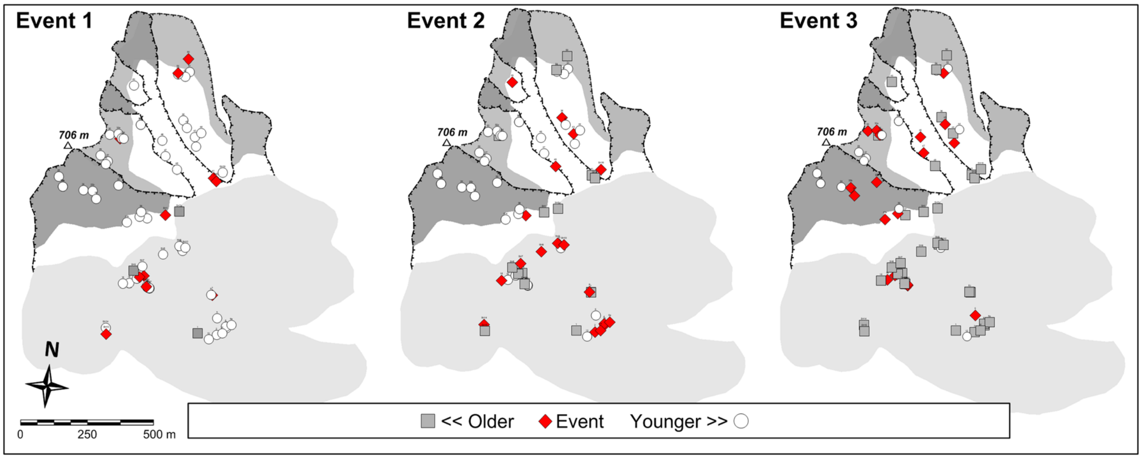

Fig. 10 Spatial distribution of sampling sites associated to particular events

cannot be excluded that the maximum age of the oldest slope deformations may be higher.

The spatial distribution of sampling sites assigned to these events is evident in Fig. 10. Individual events are always represented by clusters of points (11–20), which oscillate around major climate fluctuations at the end of the Pleistocene and Holocene (Rasmussen et al. 2006). Both events 1 and 2 could be associated with warming in the Bølling oscillation between the Oldest Dryas and Older Dryas stadials, and with warming in Younger Dryas (11,700 yBC) at the end of the last glacial period. Per our assumptions, event 3 is of a Holocene age, possibly associated with climate fluctuation in Atlantic (8200 yBC). Especially for events 2 and 3 (see Fig. 9), we hypothesize that they may be several mass movement events (a possible example could be event 2.1, which could be associated with the end of the Intra-Allerød Cold Period (ICAP)) acquired in a short interval (in hundreds of years), which cannot be further specified by timeline correlations based on Schmidt hammer testing. Of course, all of the events have a considerable time span; however, they are related to climatic fluctuations, because we assume that ideal climatic conditions occurred during these periods for the emergence of such extensive slope deformations. Inter alia, this assumption was partly supported by a pedological analysis that suggested stratigraphic break in sedimentation of all three sampled horizons.

According to this rough age estimation, the large gneiss block accumulation (*R* values 50–52) described above comes from event 2 (more precisely from its second epoch—event 2.2). These gneissic blocks are at the base of the accumulation (Fig. 4) and are the largest blocks identified during our fieldwork. We assume that the main and range-largest recorded event was event 2, and this can be linked to climate change (warming) at the end of the Younger Dryas. The accumulation at Šibeniční Hůrka (286 m a.s.l.) may be older, but it cannot be documented because it was completely excavated. Similarly, the youngest sediments close to the surface were excavated in the 1970s and early 1980s, which is why the youngest rock outcrops in the western scarp area have no equivalent in the accumulation zone.

Conclusions

A large rockslide-rock avalanche geological model in the Krušné Hory Mts. was reconstructed by the analysis of 216 geological boreholes and by GIS analysis of the pre-mining landscape. The relative age of the rocks in the head scarp and relict material of the accumulated blocks as well as the rough age was estimated by Schmidt hammer testing.

The total volume of the Quaternary sediments was calculated to be between 25.4 and 27.4 mil m^3, which is consistent with the conclusions of earlier studies from the 1970s and 1980s. This accumulation covers an area of 778,000 m^2 and its majority is the product of repeated rockslide-rock avalanches and fluently passes into layers of several (6–8) generations of colluvial sediments at the foothills of the Krušné hory Mts. The rockslide scarp area (approximately 161,000 m^2) is located on the 20°–40° steep fault slopes of Mt. Jezeř (706 m a.s.l.) and Mt. Jánský (738 m a.s.l.). We assume that the initial rocksliding passed into a debris avalanche when the rockslide material struck the water-saturated sediments of the Most Basin and so the material ran out up to 1000 m from the mountain foothills.

Three main landslide events were identified based on extensive Schmidt hammer sampling. For these events, similar *R* values were found on the sampling objects placed both in the head scarp area and the accumulation zone. These documented events can be understood as rapid landslide periods with various different extents. The approximate age of these events was estimated using the regression equation assembled by Engel (2007). According to this rough estimation, the oldest event occurred as a result of the Oldest Dryas warming. The largest event probably occurred at the end of the Younger Dryas (11,700 yBP), whereby the movements most probably occurred continuously during the Bølling-Allerød temperature fluctuations. The youngest documented event was purely of a Holocene age, with probably the highest landslide frequency during the Atlantic temperature fluctuations (approximately 8200 yBP). All three documented events oscillated around significant climate changes associated with rapid warming or sudden cooling—warming periods. In general, these periods were ideal for the evolution of large landslides besides the general geographic and climate aspects, also the specific regional conditions featured ideal conditions for large runout landslide evolution—the fault slope with the largest relative height (over 400 m) is tectonically weakened (high density of foliation, cracks, and faults with a gradient of 50°–70 and in the same direction as the main structural fault of the Kuršné hory Mts.). Sediments in the Most Basin were deeply watered during rapid warming periods, which allowed mobilization of rockslide deposits and runout up to 1000 m form the mountain foothills.

Evidence of significantly older events was not uncovered (although it certainly cannot be ruled out), as the scarp area was rejuvenated by younger events. Evidence of younger events was practically only found in the head scarp area, most probably as the younger deposits in the accumulation area were excavated by surface mining in the 1960s–1980s. Based on the Schmidt hammer age regression, we can state that this major rockslide-rock avalanche event was approximately 5–10 thousand years younger than the estimates given in the earlier studies.

References

Balatka B, Kalvoda J (2006) Geomorfologické členění reliéfu Čech. Kartografie Praha, Praha, p 79

Betts MW, Latta MA (2000) Rock surface hardness as an indication of exposure age: an archaeological application of the Schmidt hammer. Archaeometry 42:209–223

Černá B, Engel Z (2011) Surface and sub-surface Schmidt hammer rebound value variation for a granite outcrop. Earth Surf Process Landf 36:170–179

Copons R, Vilaplana JM, Linares R (2009) Rockfall travel distance analysis by using empirical models (Solà d' Andorra la Vella, Central Pyrenees). Nat Haz Earth Syst Sci 9:2107–2118

Crandell DR (1989) Gigantic debris avalanche of Pleistocene age from ancestral Mount Shasta Volcano, California, and debris-avalanche hazard zonation. USGS Bull 1861:32

Domácí L (1977) Litostratigrafie třetihorních sedimentů v hnědouhelné severočeské pánvi. Acta Univ Carol Geol 1:75–80

Engel Z (2007) Measurement and age assignment of intact rock strength in the Krkonoše Mountains, Czech Republic. Z Geomorphol 51:69–80

Goudie AS (ed) (2004) Encyclopedia of geomorphology. Vol. 1. Routledge, London, p 1184

Goudie AS (2006) The Schmidt hammer in geomorphological research. Prog Phys Geogr 30:703–718

Grygar T, Mach K (2013) Regional chemostratigraphic key horizons in the macrofossil-barren siliciclastic lower Miocene lacustrine sediments (Most Basin, Eger Graben, Czech Republic). Bull Geosci 88(3):557–571

Hartvich F, Blahut J, Stemberk J (2017) Rock avalanche and rock glacier: a compound landform study from Hornsund, Svalbard. Geomorphology 276:244–256

Hurník S (1986) Geologická problematika Velkolomu Československé armády. Zpravodaj SHR 3:28–49

Jankovská V (1983) Palynologische Forschung am ehemaligen Komořany-See (Spätglazial bis Subatlantikum). Věstník Ústředního ústavu geologického 58 (2):99–107

Jankovská V (1987) Vývoj vegetace na Mostecku na základě pylových analýz sedimentů Komořanského jezera. In: Severočeská příroda 20:113

Kalvoda J (1995) Geomorphological analysis of levelling measurements between Mikulovice village and Jezeri Castle in the Krusne Hory Mountains. Acta Univ Carol Geogr 30, Supplem.:139–160

Kalvoda J, Stemberk J, Vilímek V, Zeman A (1990) Analysis of levelling measurements of the Earth's surface movements on the geodynamic polygon Mikulovice - Jezeří in the Krušné hory Mts. Proc. 6th Int. IAEG Cong., 6–10 August 1990 Amsterdam, 3, 1631–1637, Balkema, Rotterdam, Brookfield

Kalvoda J, Vilímek V, Zeman A (1994) Earth's surface movements in the hazardous area of Jezeří kastle, Krušné hory Mts. GeoJournal 32(3):247–252

Klimeš J, Vilímek V, Omelka M (2009) Implications of geomorphological research for recent and prehistoric avalanches and related hazards at Huascaran, Peru. Nat Hazards 50(1):193–209

Kopecký A (1989) Neotektonika severočeské hnědouhelné pánve a Krušných hor. Sbor Geol Věd Geol 44:155–170

Král V (1968) Geomorfologie vrcholové části krušných hor a problém paroviny. Rozpravy Československé akademie věd 78(9):42–49

Malkovský M (1977) Důležité zlomy platformního pokryvu severní části Českého masívu. Ústř Úst Geol 14:7–12

Malkovský M (ed) (1985) Geologie Severočeské hnědouhelné pánve a jejího okolí. Academia, Praha, p 424

Marek J (1979) Šibeniční hůrka u Dřínova před odtěžením. Uhlí 27(11):498–501

Marek J (1983) Inženýrsko-geologický průzkumu stability zámku Jezeří v předpolí uhelného velkolomu. Geolog Průzk 25:234–236

Němčok A, Pašek J, Rybář J (1972) Classification of landslides and other mass movements. Rock Mech 4:71–79

Okada Y, Uchida I (2014) Dependence of runout distance on the number of rock blocks in large-scale rock-mass failure experiments. J For Res 19(3):329–339

Rasmussen SO, Andersen KK, Svensson AM, Steffensen JP, Vinther BM, Clausen HB, Siggaard-Andersen M-L, Johnsen SJ, Larsen LB, Dahl-Jensen D, Bigler M, Röthlisberger R, Fischer H, Goto-Azuma K, Hansson ME, Ruth U (2006) A new Greenland ice core chronology for the last glacial termination. J Geophys Res Atmos 111(6):2156–2202

Růžičková E, Zeman A, Hurník S (1987) Vývoj jihovýchodního okraje Krušných hor a Mostecké pánve v mladším kenozoiku. Sbor Geol Věd, Ř A 18:9–72

Rybář J (1981) Inženýrsko-geologické hodnocení stabilitních poměrů předpolí povrchových velkolomů při úpatí Krušných hor. Stabilitní řešení svahů a jejich zabezpečení, Sborník přednášek semináře, Most, pp, 76–93

Sánchez SJ, Mosquera DF, Vidal Romaní JR (2009) Assessing the age-weathering correspondence of cosmogenic 21Ne dated Pleistocene surfaces by the Schmidt hammer. Earth Surf Process Landf 34:1121–1125

Sartori M, Baillifard F, Jaboyedoff M, Rouiller J-D (2003) Kinematics of the 1991 Randa rockslides (Valais, Switzerland). Nat Hazards Earth Syst Sci 3:423–433

Schlesinger L (1871) Festschrift zur Erinnerung an die Feier des 10. Gründungstages im Jahre 1871. Geschichte des Kummerner Sees bei Brüx, Praha, p 26

Selby MJ (1980) A rock–mass strength classification for geomorphic purposes: with tests from Antarctica and New Zealand. Z Geomorphol 24:31–51

Shakesby RA, Matthews JA, Owen G (2006) The Schmidt hammer as a relative-age dating tool and its potential for calibrated-age dating in Holocene glaciated environments. Quat Sci Rev 25:2846–2867

Špůrek M (1974) Sesuvné jevy u Dřínova na Mostecku. Věst Ustř Úst Geol 49:231–234

Stoffel M (2005) Spatio-temporal variations of rockfall activity into forests—results from tree-ring and tree analysis, University of Fribourg. GeoFocus 12:188

Strom KE, Abdrakhmatov KE (2016) Rock slides and rock avalanches of the Kokomeren River basin (Central Tien Shan). ICL Summer School Guidebook, IPL project, http://iplhq.org/icl/, p 131

Váně M (1960) Debris and landslides at the foot of the krušné hory Mts. Čas Min Geol 5(2):174–177

Váně M (1985) Geologická stavba podkrušnohorského prolomu a jeho tektogeneze. Sbor Geol Věd, Geologie 40:147–181

Viles HA, Goudie AS, Grab S, Lalley J (2011) The use of the Schmidt hammer and Equotip for rock hardness assessment in geomorphology and heritage science: a comparative analysis. Earth Surf Process Landf 36(3):320–333

Vilímek V (1995) Quaternary development of Kateřinohorská Vault relief in the Krušné hory mountains. Acta Universitatis Carolinae, Geographica 30, Supplem:115–137

Zapletal L (1954) Zbytky Komořanského jezera. Ochrana přírody 9(2):57–58

Zmítko J (1983) Fosilní sesuvy při podkrušnohorském výchozu pánve. Zpravodaj Hnědé uhlí 6:12–24

J. Burda · M. Veselý · M. Řehoř
Brown Coal Research Institute j.s.c.,
Tř. Budovatelů 2830/3, Most, Czech Republic

J. Burda
e-mail: burda@vuhu.cz

V. Vilímek (✉)
Faculty of Science,
Charles University,
Albertov 6, Prague 2, Czech Republic
e-mail: vilimek@natur.cuni.cz